ISSN 0021-891X, Volume 40, Number 4

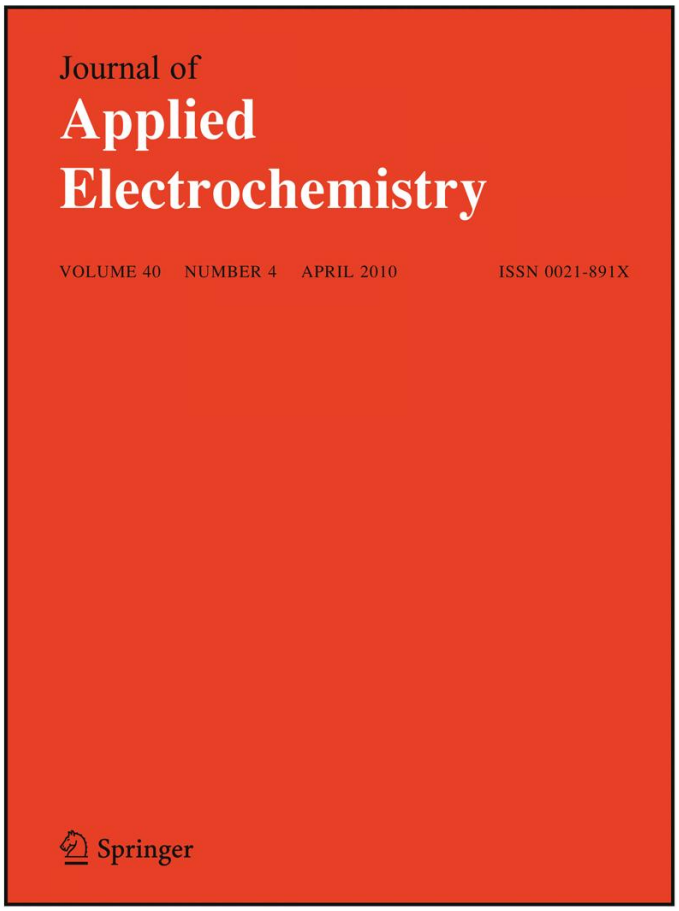

J Appl Electrochem (2010) 40:719–727
DOI 10.1007/s10800-009-0049-2

ORIGINAL PAPER

A novel IrO_2 electrode with iridium–titanium oxide interlayers from a mixture of TiN nanoparticle and H_2IrCl_6 solution

Hai-Bo Xu · Yong-Hong Lu · Chun-Hu Li · Jie-Zhen Hu

Received: 18 August 2009 / Accepted: 1 December 2009 / Published online: 15 December 2009

Abstract A novel IrO_2 anode on titanium substrate with iridium–titanium oxide interlayer (Ti/IrO_x–TiO_2/IrO_2) was prepared and investigated for oxygen evolution. IrO_x–TiO_2 interlayer was coated on titanium substrate by impregnation-thermal decomposition method from a mixture of TiN nanoparticles and H_2IrCl_6 solution at 500 °C. The results showed that the service life of Ti/IrO_x–TiO_2/IrO_2 was a factor of six times longer than that of Ti/IrO_2, which was attributed to the IrO_x–TiO_2 interlayer, it could form a metastable solid solution between IrO_x and thin titanium oxide layer on titanium substrate during calcination. The interlayer contributed to the decrease in migration rate of oxygen atom or molecule toward substrate and the increase in bonding force among IrO_2 layer, interlayer, and substrate. Therefore, besides keeping high electrocatalytic activity, the service life of Ti/IrO_x–TiO_2/IrO_2 electrode was greatly improved, and its overall electrocatalytic performance for oxygen evolution was increased as well.

Keywords Titanium nitride · Iridium oxide · Titanium oxide · Interlayer · Dimensional stable anode (DSA) · Service life

1 Introduction

Rutile IrO_2 behaves like a metal material, which has a high electronic conductivity at room temperature, thereby it is widely used as O_2 and Cl_2 evolution electrode, oxidation resistance coating and pH sensor material [1–6]. In the past decades, IrO_2-based metallic oxide catalysts for oxygen evolution have attracted much attention. Normally, IrO_2 is regarded as a very stable and excellent metallic oxide in acidic solutions with high electrocatalytic activity and corrosion resistance for oxygen evolution [7–9]. Used as an electrode, IrO_2 is generally coated on titanium substrate, forming a traditional dimensional stable anode (DSA). However, except the advantage of low oxygen-evolution overpotential, the stability of Ti/IrO_2 electrode is not satisfying. The deterioration of titanium substrate easily occurs at high current density in corrosive electrolytes, such as in H_2SO_4 solution, shortening the service life of electrode. Moreover, oxygen-evolution overpotential and corrosion rate of Ti/IrO_2 electrode can be unfavorably increased in electrolytes containing organic species [10].

In order to increase the lifetime and decrease the cost of coating, some non-conductive stabilizing agents are necessarily added. In general, Ta_2O_5, TiO_2, ZrO_2, and SnO_2 are used as stabilizing or dispersing components in IrO_2-coated DSA [11–18]. A Ti/IrO_2–Ta_2O_5 electrode (7:3 molar ratio of Ir/Ta) has been reported to present the highest electrocatalytic activity and the longest service life in acidic media [19].

In addition, the service life of Ti/IrO_2 can also be improved by adding interlayers, such as tantalum, tin, and titanium metallic oxide or nitride, etc. [20–22]. The interlayer can prevent or delay the oxygen atom or molecule penetrating into the titanium substrate, and consequently protect the substrate from corrosion. However, there are still some disadvantages. On the one hand, the different preparation methods for interlayer and IrO_2 coating lead to a very complicated preparation process; on the other hand, the interfaces among titanium substrate, interlayer and IrO_2

H.-B. Xu (✉) · Y.-H. Lu · C.-H. Li · J.-Z. Hu
Key Laboratory of Marine Chemistry Theory and Technology, Ministry of Education, College of Chemistry and Chemical Engineering, Ocean University of China, Qingdao 266100, China
e-mail: xuwangri@163.com

coating are probably lack of gradient changes in composition and structure, resulting in a limited bonding force.

In our previous work [23], a nano-scale IrO_x–TiO_2 powder with a 1:6.5 atomic ratio of Ir/Ti had been synthesized from TiN nanoparticle precursors via impregnation-thermal decomposition method. In this binary oxide, TiO_2 served as a dispersing agent, and IrO_x as an active material; its good conductivity and high homogeneous dispersion with metastable solid solution characteristic made IrO_x–TiO_2 superior to IrO_2 for oxygen-evolution process [23]. On the base of nano-scale IrO_x–TiO_2 catalyst, we prepared a new Ti/IrO_x–TiO_2/IrO_2 electrode with IrO_x–TiO_2 as interlayer, using the same preparation method for interlayer and surface layer to avoid the complicated preparation process. Here, interlayer acted as a gradient layer in composition and structure, to expect the comparable catalytic activity and longer durability for new electrode in H_2SO_4 solution. In this article, compared with the traditional Ti/IrO_2 electrode, electrochemical performance and physical characterization of novel Ti/IrO_x–TiO_2/IrO_2 electrode were investigated, and the possible reasons were tried to be explained.

2 Experimental

2.1 Powder preparation

To compare the function of TiN nanoparticle in precursor solution, sample A was prepared by heating 1 g TiN nanoparticles (99%, 20 nm, HFKILN China) at 500 °C in air atmosphere for 2 h. At the same time, sample B was prepared with the following procedure: impregnating 1 g TiN nanoparticles into a mixture of 16 mL *n*-butanol and 2 mL hydrochloric acid (37 wt%) (here it was called TiN nanoparticle precursor solution without H_2IrCl_6), dried at 120 °C for 3 h to allow solvent vaporize, then calcining at 500 °C in air atmosphere for 2 h, finally TiO_2 nanoparticles were obtained.

2.2 Electrode preparation

Prior to an experiment, a commercial TA2 titanium plate (25 × 25 × 2 mm), used as the substrate of oxide coating, was degreased and etched in a 10 wt% oxalic acid solution at 98 °C for 3 h, and then cleaned in deionized water.

Sample C was prepared with the following procedure: obtaining the same TiN nanoparticle precursor solution without H_2IrCl_6 as sample B, brushing this solution on a titanium plate, drying at 120 °C for 10 min, then calcining at 500 °C in air atmosphere for 15 min. The processes of brushing, drying, and calcinating were repeated again to obtain the Ti/TiO_2 electrode coated two times (sample C).

H_2IrCl_6 solution was prepared by dissolving 2 mL $H_2IrCl_6{\cdot}6H_2O$ (35 wt% Ir, from PGMCHINA) into a mixture of 13.9 mL *n*-butanol and 2 mL hydrochloric acid (37 wt%), which was used as the coating solution. TiN nanoparticle precursor solution with H_2IrCl_6 was prepared by mixing 32 mg TiN nanoparticles into 2 mL H_2IrCl_6 solution described above. Prior to coating, the precursor solution was ultrasonically dispersed for 1 h.

Thermal decomposition method was employed to prepare the oxide interlayer and coating. Titanium plate was brushed with TiN nanoparticle precursor solution with H_2IrCl_6 at room temperature, dried at 120 °C for 10 min, and then calcined at 500 °C for 15 min; repeating brushing–drying–calcinating procedure with required times to obtain the IrO_x–TiO_2 interlayer.

Comparing electrocatalytic and stable performance of IrO_x–TiO_2 interlayer coated twice with that coated more times, the former was better. This could be attributed to more TiO_2 in IrO_x–TiO_2 interlayer coated more times, leading to less conductivity of interlayer, hence all interlayers were prepared by coating twice later. This Ti/IrO_x–TiO_2 electrode was used as sample D.

Following that, on IrO_x–TiO_2 interlayer, a brushing H_2IrCl_6 solution–drying–calcinating procedure was repeated three times to obtain Ti/IrO_x–TiO_2/IrO_2 coating electrode (sample E-1, totally coated five times). Sample E-2 was prepared by the same procedure as E-1 until total oxide loading was about 10 g m^{-2}, generally repeating 18 times (totally coated 20 times). For comparison, two Ti/IrO_2 electrodes (samples F-1 and F-2) were prepared by the same procedure as samples E-1 and E-2 except no interlayer, i.e., brushing H_2IrCl_6 solution five times and 20 times, respectively, directly on titanium plate.

Finally, all samples were annealed at 500 °C for 1 h.

2.3 Electrochemical measurement

Anodic polarization curve was measured by using a conventional three-electrode cell in 0.5 mol dm^{-3} H_2SO_4 solution at room temperature. Ti/IrO_x–TiO_2/IrO_2 coating electrode (sample E-2) and Ti/IrO_2 electrode (sample F-2) were used as anode, respectively, both with a 1 cm^2 working area. A 4 cm^2 platinum sheet and a saturated calomel electrode (SCE) were used as cathode and reference electrode. All potentials reported here were referred to SCE.

Before polarization tests, solution ohmic resistance (R_s) was measured by electrochemical impedance spectrum (EIS) at open circuit potential, which was the value of the real part of impedance measured at the highest frequency. Polarization curves were corrected by subtracting the solution ohmic drop. An EG&G PAR Model 2263 Potentiostat/Galvanostat controlled by PowerSuite software was

used for polarization and EIS measurements. Polarization tests were carried out from open circuit potential in a positive-going sweep at the scan rate of 1 mV s^{-1}.

2.4 Physical characterization

Surface morphology of electrodes was observed with a scanning electron microscope (SEM; XL30, Philips), including titanium substrate etched by a 10 wt% oxalic acid solution, samples C, D, E-1, F-1, E-2, and F-2 before deterioration, as well as samples E-2 and F-2 after deterioration, respectively. Surface composition of samples E-2 and F-2 after deterioration was examined by energy-dispersive spectrometry (EDS; PHOEN IX, Edax). X-ray diffraction (XRD) patterns of electrodes were measured using a Cu Kα radiation system (40 kV, 100 mA, 6°min^{-1}, D8 ADVANCE, BRUKER), including titanium substrate etched by a 10 wt% oxalic acid solution, titanium substrate etched and then heated at 500 °C in air atmosphere, samples A, B, C, D, E-2, and F-2.

2.5 Accelerated life test

Electrochemical durability of coatings, on a laboratory scale, was evaluated by accelerated life test [24]. A 10 × 10 × 2 mm test sample cutting from a large area coating used as a working electrode was installed on a titanium clamp. A titanium plate with large area was used as a counter electrode. Cell voltages of samples E-1 and F-1 were detected as a function of time for galvanostatic electrolysis at 2.0 A cm^{-2} in 2.0 mol dm^{-3} H_2SO_4 solution at 30 °C, whereas cell voltages of samples E-2 and F-2 were detected at 3.0 A cm^{-2} in 4.0 mol dm^{-3} H_2SO_4 solution at 30 °C in order to reduce the test time. A dc power supply was used to provide a constant current. Here, the service life of an electrode was defined as the total electrolysis time before cell voltage was below 5.0 V under above operating conditions.

In order to compare the corrosion resistance, electrolysis process was interrupted for 12 h every time, once for sample F-2 at ca. 190 h, twice for sample E-2 at ca. 190 h and 440 h. Electrodes were still immerged in H_2SO_4 solution during interrupted power.

3 Results and discussion

3.1 SEM images

Figure 1a showed typical scanning electron micrographs for freshly etched titanium substrate. It was characterized by the presence of pockmarks, which could increase bonding force between active material and substrate metal [25]. Figure 1b (sample C) showed a porous titanium substrate with a number of granulated agglomerates settled in pockmarks, which were TiO_2 coming from TiN oxidation. It was a pity that a part of pockmarks could not be filled with TiN nanoparticles due to the ununiformity by manual brushing. After loading iridium oxide catalyst, Fig. 1c (sample D) indicated that the granulated agglomerates connected together into a smooth layer with some mud-cracks and small catalyst particles dispersing on surface, which was in agreement with previous report for IrO_2 electrode [26, 27].

Typical mud-cracks were also observed in Fig. 2a, b (sample F-1, sample E-1), which generally provide the space for smooth release of oxygen bubbles. Compared Fig. 2a with Fig. 2b, the cracks on surface of sample E-1 not only became relatively narrow and shallow, but also increased in number, with well-grown crystallites dispersing more uniformly.

After brushing more times, the mud-cracks on Ti/IrO_x–TiO_2/IrO_2 coating became inconspicuous, and its surface morphology was very similar to that of Ti/IrO_2 coating, with a granular-like morphology consisting of innumerable small crystallites and micropores, as shown in Fig. 3a, b. This structure could effectively block oxygen atom or molecule penetrating into the titanium substrate, and was in favor of a larger surface area as electrode material. Compared with Ti/IrO_2 coating, micropores on surface of Ti/IrO_x–TiO_2/IrO_2 coating were smaller, IrO_2 crystallite grains were more uniformly dispersed, and its average crystal size was finer.

3.2 XRD analysis

Figure 4a showed the XRD pattern of titanium substrate etched in 10 wt% oxalic acid. In addition to titanium metal peaks from the substrate, titanium hydride peaks were also present. After heated in air atmosphere at 500 °C, titanium hydride was decomposed, and rutile TiO_2 was formed on titanium substrate, as shown in Fig. 4b.

Figure 4c showed the XRD pattern of TiO_2 powder made from TiN nanoparticle heated in air atmosphere at 500 °C (sample A). XRD analysis indicated that the powder was mainly composed of anatase TiO_2 with a small quantity of rutile TiO_2 present. However, after impregnating TiN nanoparticles with a mixture of *n*-butanol and hydrochloric acid and heated at 500 °C (sample B), rutile TiO_2 was predominantly formed (see Fig. 4d), revealing that alcoholic solvent benefited the phase transformation of TiO_2. Moreover, after coating the same TiN nanoparticle precursor solution as sample B on etched titanium plate to obtain Ti/TiO_2 electrode (sample C), its XRD result (see Fig. 4e) was similar to Fig. 4d, indicating that TiN could be converted into rutile TiO_2.

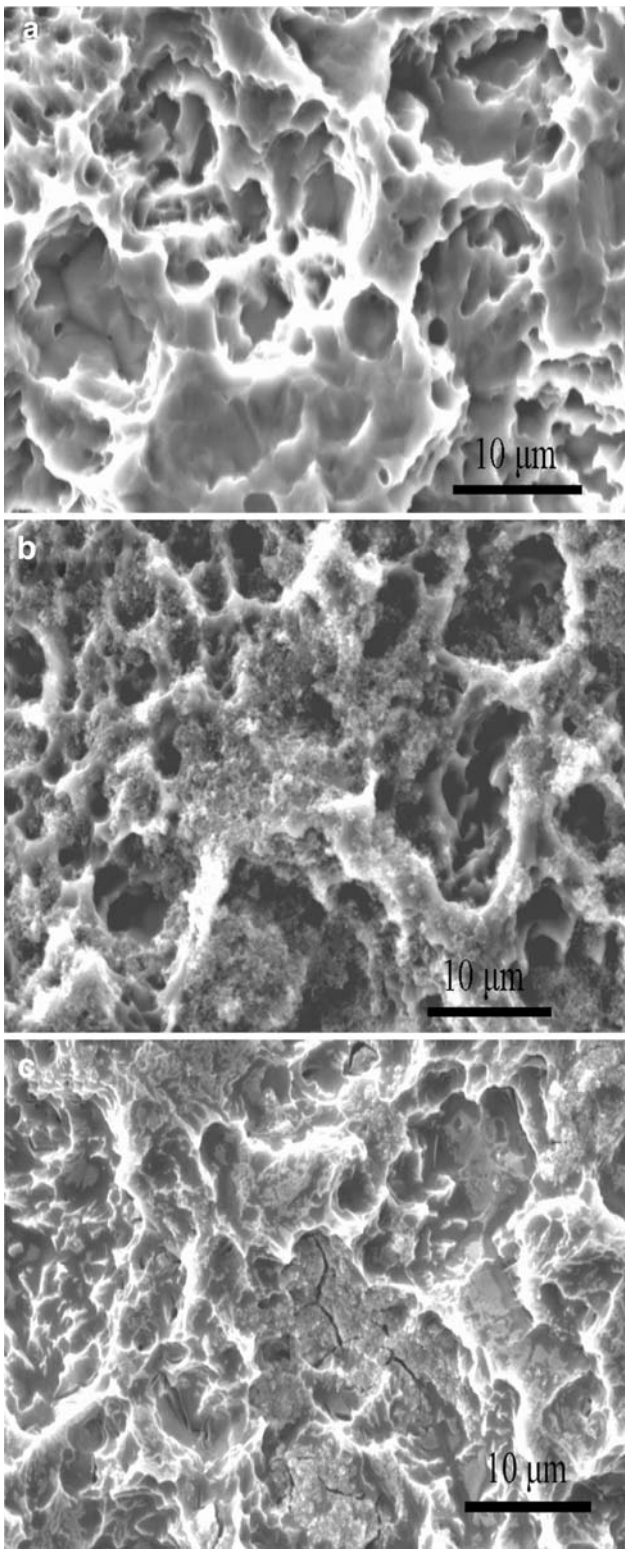

Fig. 1 Scanning electron micrographs of coating surfaces. **a** Titanium substrate etched by a 10 wt% oxalic acid solution, **b** Ti/TiO_2 electrode coated two times (sample C), and **c** Ti/IrO_x–TiO_2 electrode coated two times (sample D). Magnification: ×5,000

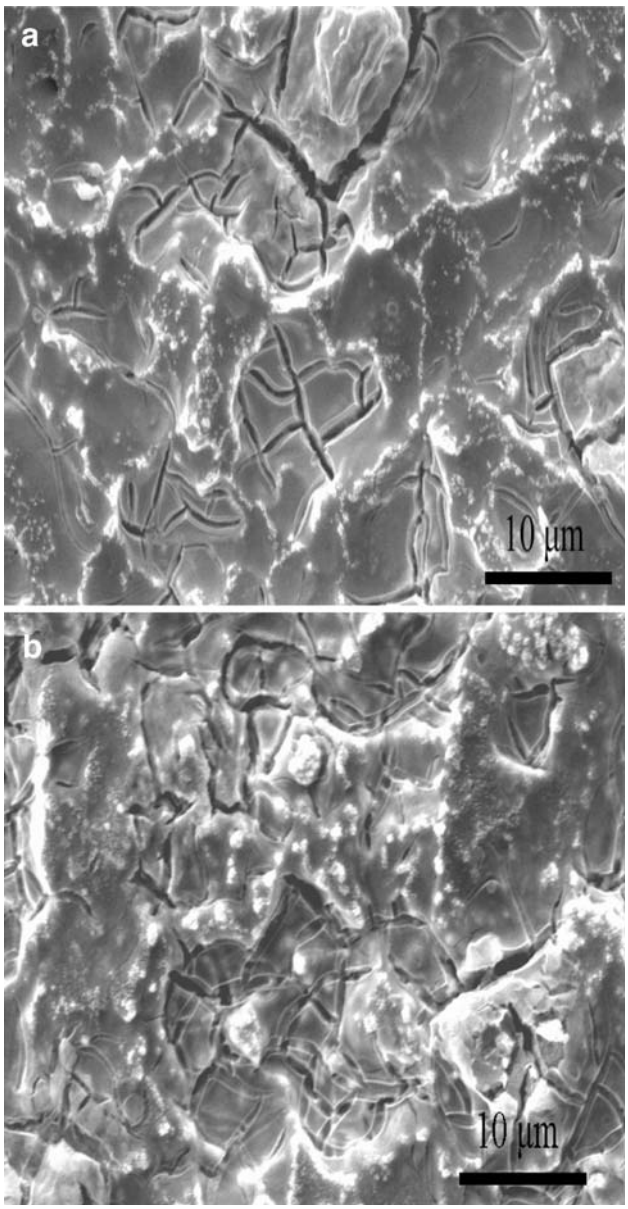

Fig. 2 Scanning electron micrographs of coating surfaces. **a** Ti/IrO_2 electrode coated five times (sample F-1), **b** Ti/IrO_x–TiO_2/IrO_2 coating electrode coated five times (sample E-1). Magnification: ×5,000

Figure 4f showed XRD pattern of sample D with IrO_x–TiO_2 coated on etched titanium substrate. In addition to titanium metal peak from substrate, other two broad and symmetric IrO_2 peaks were found. Judging from peak positions, they corresponded with the rutile structure, indicating that TiO_2 and IrO_2 formed a binary solid solution in a rutile phase [26].

Similar XRD patterns of Ti/IrO_2 (samples F-2) and Ti/IrO_x–TiO_2/IrO_2 (sample E-2) were shown in Fig. 5a, b. Compared with Fig. 5a, b revealed that the addition of

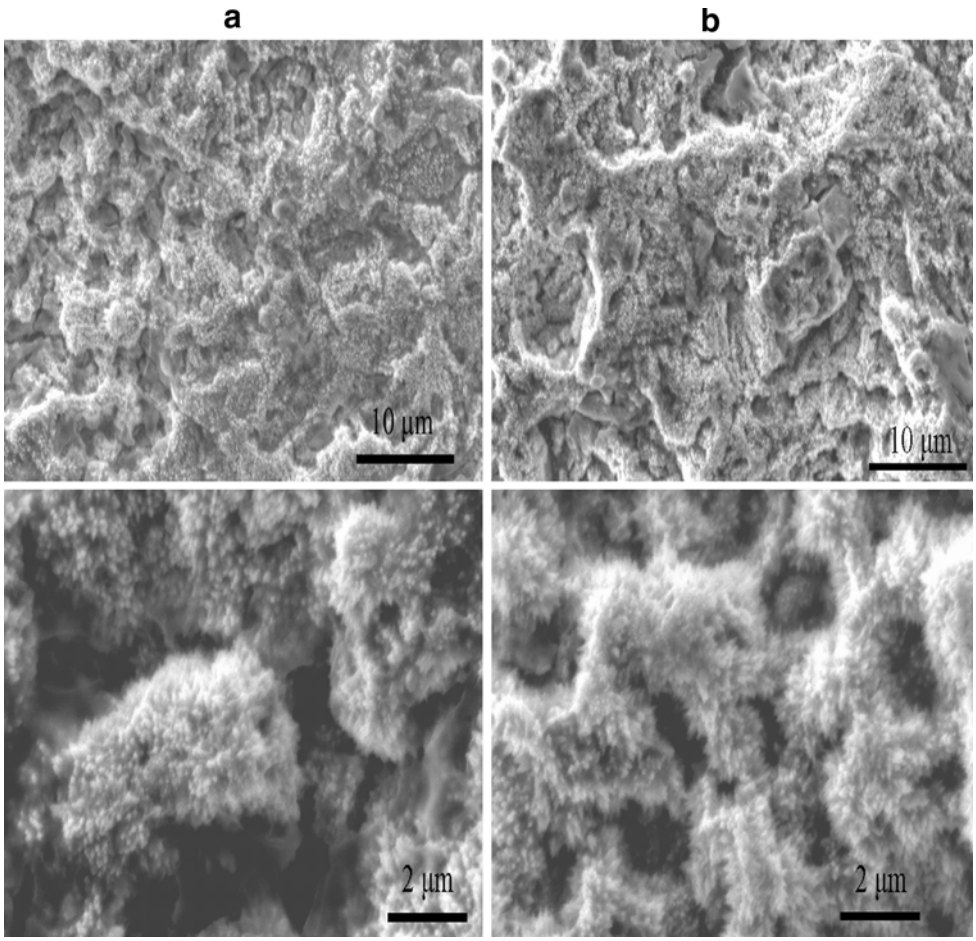

Fig. 3 Scanning electron micrographs of coating surfaces. **a** Ti/IrO_2 coated 20 times (sample F-2), **b** Ti/IrO_x–TiO_2/IrO_2 coated 20 times (sample E-2). Top two (low magnification): ×5,000, bottom two (high magnification): ×20,000

IrO_x–TiO_2 interlayer did not change the phase structure of IrO_2 coating. Therefore, addition of IrO_x–TiO_2 interlayer was probably prone to forming a metastable solid solution between titanium oxide layer on etched titanium substrate and IrO_2 active surface during calcination.

Average crystal size of rutile grains in Ti/IrO_x–TiO_2/IrO_2 coating (sample E-2) was 14.9 nm (see Fig. 5b) and 17.5 nm (see Fig. 5a) in Ti/IrO_2 coating (sample F-2), calculated by means of the Scherrer equation [28], agreeing with the surface micrographs of coatings (see Fig. 3a, b).

3.3 Polarization behavior

Figure 6 showed the anodic polarization curves of Ti/IrO_2 (sample F-2) and Ti/IrO_x–TiO_2/IrO_2 (sample E-2) electrodes in 0.5 mol dm^{-3} H_2SO_4 at room temperature. Electrocatalytic characteristic of Ti/IrO_x–TiO_2/IrO_2 electrode was nearly the same as that of Ti/IrO_2, but its oxygen-evolution potential was apparently lower than that of Ti/IrO_2 over examined current densities range. Therefore, overall electrocatalytic activity of Ti/IrO_x–TiO_2/IrO_2 electrode was improved after adding interlayer.

Considering surface morphology and polarization behavior of Ti/IrO_x–TiO_2/IrO_2 electrode, its high electrocatalytic activity could be correlated with slightly finer crystals and more uniform dispersion of IrO_2 particles on coating surface [29].

3.4 Accelerated life test

To compare the electrochemical stability, accelerated life tests were performed for Ti/IrO_x–TiO_2/IrO_2 (sample E-1) and Ti/IrO_2 (sample F-1) electrodes, shown in Fig. 7. Ti/IrO_x–TiO_2/IrO_2 electrode showed a six times longer service life than that of Ti/IrO_2, with the former lasting about 135 h whereas the latter only 22 h. It indicated that the electrochemical stability of Ti/IrO_x–TiO_2/IrO_2 electrode was far superior to that of Ti/IrO_2 under the same conditions.

In addition, the increment in coating thickness was also an effective way to obtain a long service life for IrO_2 electrode, and increasing coating times could do this and decrease the surface cracks [24]. Figure 8 showed the accelerated life tests for Ti/IrO_x–TiO_2/IrO_2 (sample E-2)

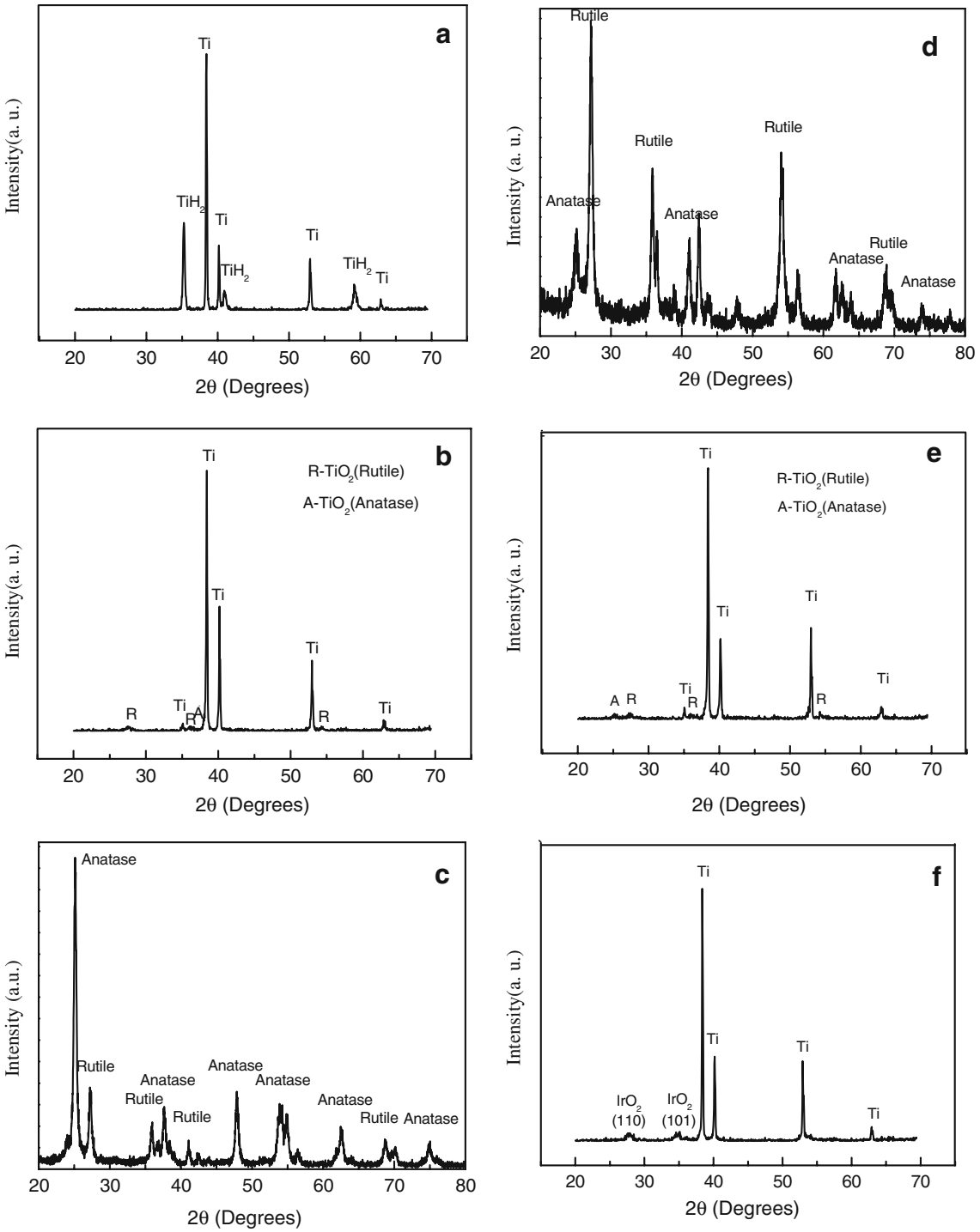

Fig. 4 XRD patterns of titanium substrate, powders, and electrode coating. **a** Titanium substrate etched in 10 wt% oxalic acid, **b** titanium substrate etched and then heated at 500 °C in air, **c** TiO_2 powder from TiN nanoparticle heated at 500 °C (sample A), **d** TiO_2 powder from TiN nanoparticle precursor solution without H_2IrCl_6 heated at 500 °C (sample B), **e** Ti/TiO_2 coated two times (sample C), and **f** Ti/IrO_x–TiO_2 coated two times (sample D)

and Ti/IrO_2 (sample F-2) electrodes. The service life of two electrodes (coated 20 times) in Fig. 8 became obviously longer than those (coated five times) in Fig. 7. In order to compare the corrosion resistance, electrolysis process was interrupted for 12 h, once at about 190 h for Ti/IrO_2 electrode, twice at about 190 h, and 440 h for Ti/IrO_x–TiO_2/IrO_2 electrode, respectively. A sharp increase of cell voltage was observed for Ti/IrO_2 electrode after current

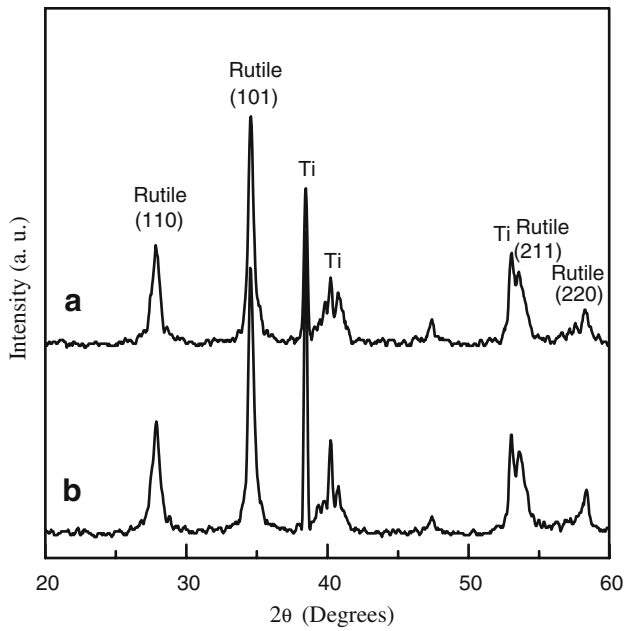

Fig. 5 XRD patterns of electrode coating. *a* Ti/IrO_2 coated 20 times (sample F-2), *b* Ti/IrO_x–TiO_2/IrO_2 coated 20 times (sample E-2)

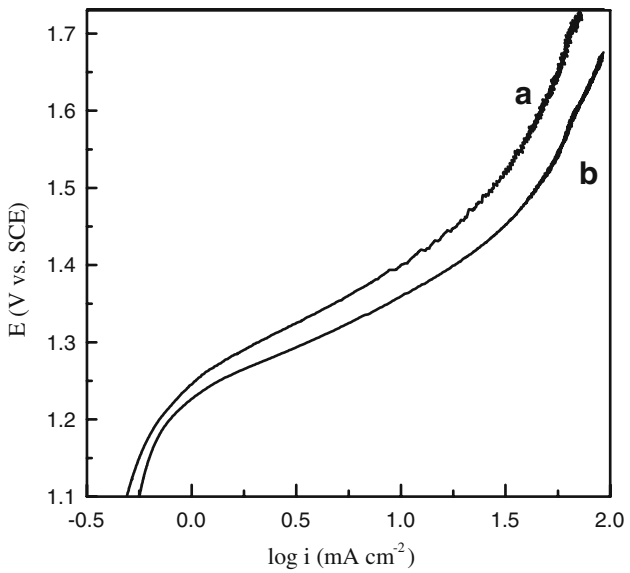

Fig. 6 Anodic polarization curves of electrodes from *a* Ti/IrO_2 coated 20 times (sample F-2), *b* Ti/IrO_x–TiO_2/IrO_2 coated 20 times (sample E-2) in 0.5 mol dm^{-3} H_2SO_4 solution. Scan rate: 1 mV s^{-1}

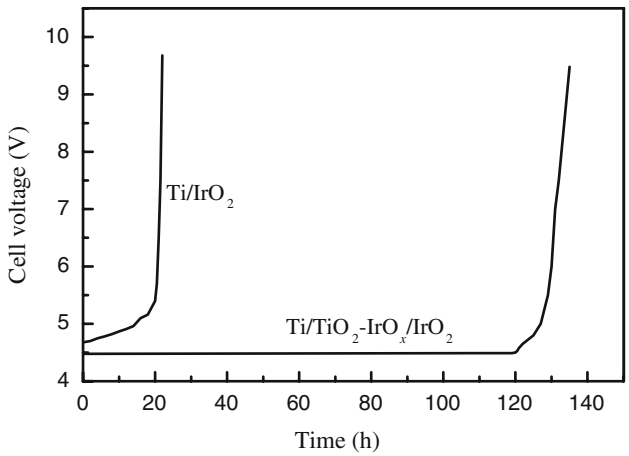

Fig. 7 Accelerated life test comparison between Ti/IrO_2 coated five times (sample F-1) and Ti/IrO_x–TiO_2/IrO_2 coated five times (sample E-1) in 2.0 mol dm^{-3} H_2SO_4 solution under 2.0 A cm^{-2} at 30 °C

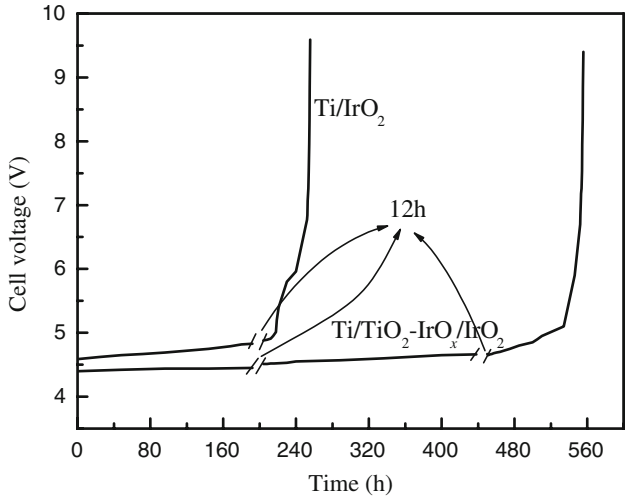

Fig. 8 Comparison of accelerated life between Ti/IrO_x–TiO_2/IrO_2 coated 20 times (sample E-2) and Ti/IrO_2 coated 20 times (sample F-2) in 4.0 mol dm^{-3} H_2SO_4 solution under 3.0 A cm^{-2} at 30 °C

was interrupted, finally lasting 256 h. This revealed the damage to titanium substrate by strong corrosive H_2SO_4 solution, so the deterioration process was accelerated. Contrarily, the cell voltage of Ti/IrO_x–TiO_2/IrO_2 electrode was not obviously changed after interrupting power, i.e., titanium substrate was resistant to corrosion owing to the presence of interlayer, finally lasting about 556 h. In a word, though Ti/IrO_x–TiO_2/IrO_2 electrode had a similar surface morphology as Ti/IrO_2 electrode, the presence of an interlayer could greatly increas the substrate protection from deterioration. However, considering the cost, coating less times seemed more profitable than more times. Therefore, it needed comprehensive evaluation between low cost and long service life.

SEM images of Ti/IrO_2 (sample F-2) and Ti/IrO_x–TiO_2/IrO_2 (sample E-2) electrodes after deterioration were shown in Fig. 9a, b. Some surface coating fell off, and titanium substrate was corroded for two electrodes. However, by comparison, coating of Ti/IrO_2 electrode was more easily lost than that of Ti/IrO_x–TiO_2/IrO_2, indicating of a good bonding force between coating and substrate for Ti/IrO_x–TiO_2/IrO_2. Moreover, at the end of the accelerated life test, EDS results for coating surface revealed that

iridium content was still high, nearly 70%; this indicated that the degradation must be attributed to substrate passivation instead of coating detachment, conforming to SEM results of Fig. 9a, b. Therefore, it was because the interfaces among titanium substrate, interlayer and surface IrO_2 layer had gradient changes in composition and structure that a strong bonding force between coating and substrate was formed.

In general, DSA coating on titanium substrate may form three kinds of different interfaces, that is, coherent interface, semi-coherent interface, and noncoherent interface. Coherent bonding could enhance the adhesive strength of the coatings [30]. Here, Ti/IrO_x–TiO_2/IrO_2 electrode was made up of a multilayered oxide coating, this might benefit the coherent epitaxial growth in respect that two materials had the same crystal structure and approximate lattice constant. Furthermore, an alternating strain field was formed in multilayers due to lattice mismatch between two coherent layers. This strain field and the different dislocation line energies of per unit length in two layers due to modulus difference inhibited the movement of dislocation, and thus strengthened the multilayers [31, 32]. Recently, it was found that metastable phases could be formed in multilayers owing to "template effect," which meant that the former deposited layer had a strong influence on crystal structure of a newly deposited layer during the growth of multilayers [33].

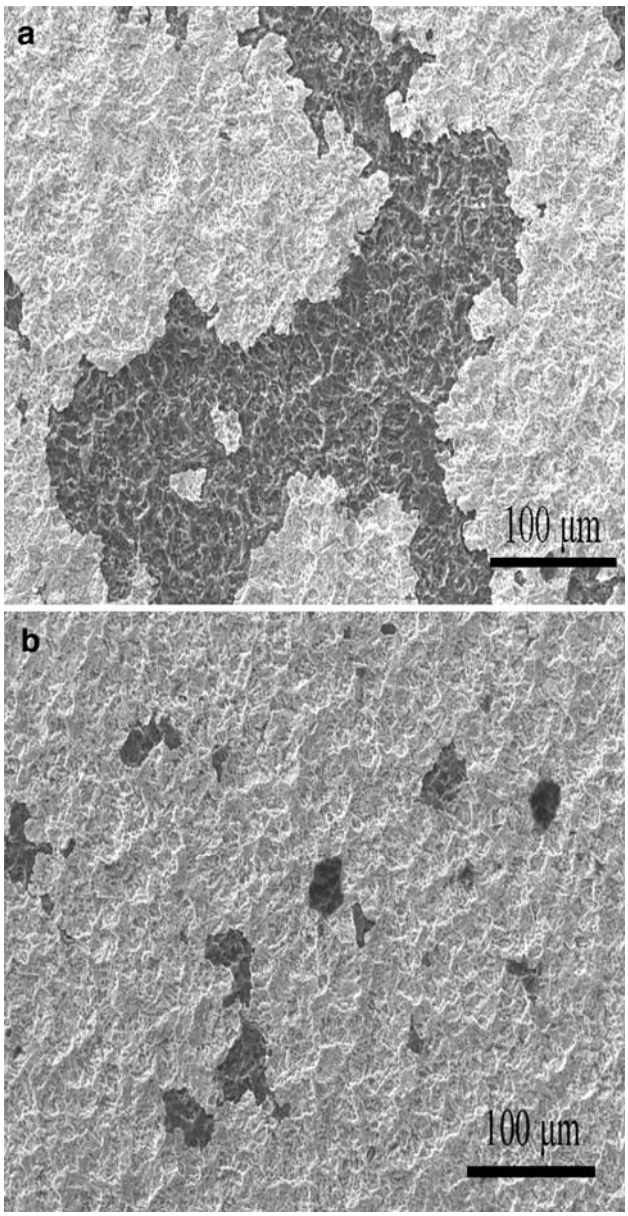

Fig. 9 SEM images of electrodes after deterioration **a** Ti/IrO_2 coated 20 times (sample F-2), **b** Ti/IrO_x–TiO_2/IrO_2 coated 20 times (sample E-2), Magnification: ×500

Next to titanium substrate, an electro-conductive thin titanium oxide layer (20–50 nm) was formed during calcination. It consisted of a mixture of TiO_2, Ti_2O_3, and TiO from substrate oxidation, even rutile TiO_2 from TiH_2 oxidation, which could protect substrate from corrosion [21]. As for a traditional Ti/IrO_2 anode, IrO_2 and TiO_2 had the same rutile structure, and approximate lattice constant (IrO_2, $a = b$, 0.4498 nm; c, 0.3154 nm; TiO_2, $a = b$, 0.4592 nm; c, 0.2958 nm); thus a coherent IrO_2–TiO_2 structure might be formed between thin titanium oxide layer and IrO_2 layer, and the multilayer was ultimately strengthened. And what is more, when TiN nanoparticle was added into the precursor solution for Ti/IrO_x–TiO_2/IrO_2 electrode, the oxidation of TiN, if it occurred, formed rutile TiO_2 and left behind a considerable structure vacancy as a consequence of nitrogen-escaping [34], which helped active material permeate mutually among titanium substrate, interlayer and surface IrO_2 layer.

It is well known that the fast migration rate of oxygen atom or molecule can accelerate the formation of a TiO_2 insulating layer between titanium substrate and coating, leading to electrode easily passivated [35]. Therefore, for Ti/IrO_2 electrode, those wide and deep cracks, made oxygen easily penetrate into titanium substrate, and its service life was eventually shortened. On contrary, the service life of Ti/IrO_x–TiO_2/IrO_2 electrode was much longer than Ti/IrO_2 electrode. On the one hand, the oxidation of TiN caused interlayer considerably expand [36], so that the surface cracks became relatively narrow and shallow. On the other hand, the formation of IrO_x–TiO_2 solid solution and coherent interface among the thin titanium oxide layer, IrO_x–TiO_2 interlayer and IrO_2 layer prevented oxygen migration.

When increasing coating times, coating thickness of Ti/IrO_2 increased, its surface morphology was gradually changed from cracks into a granular-like structure with innumerable small crystallites and micropores, which could delay the penetration of oxygen to some degree. However,

it could not resist strong corrosion from H_2SO_4 solution in accelerated life test. In contrast, Ti/IrO_x–TiO_2/IrO_2 electrode was found the excellent corrosion resistance in this study in any case. Therefore, this interlayer from TiN nanoparticle was eventually proved an effective way.

4 Conclusions

A novel titanium substrate IrO_2 anode with iridium–titanium oxide interlayer (Ti/IrO_x–TiO_2/IrO_2) was prepared and investigated for oxygen evolution by physical characterization and electrochemical tests. Moreover, the electrocatalytic activity and service life of Ti/IrO_x–TiO_2/IrO_2 electrode was compared with traditional Ti/IrO_2 electrode.

When TiN nanoparticle was introduced into the precursor solution for Ti/IrO_x–TiO_2/IrO_2 electrode, active material permeated mutually among titanium substrate, interlayer and surface IrO_2 layer; IrO_x–TiO_2 solid solution and coherent interface were formed after calcination. Therefore, compared with Ti/IrO_2 electrode, besides keeping high electrocatalytic activity, the service life of Ti/IrO_x–TiO_2/IrO_2 electrode was evidently longer. Finally, it could be concluded that overall electrocatalytic performance of Ti/IrO_x–TiO_2/IrO_2 electrode for oxygen evolution was improved after adding interlayer.

Acknowledgments This article has been supported by the Natural Science Foundation of Shandong Province of China (Y2008B25) and the National High Technology Research and development program of China (863 project, 2007AA061800).

References

1. Yoshinaga N, Sugimoto W, Takasu Y (2008) Electrochim Acta 54:566
2. Balko EN, Nguyen PH (1991) J Appl Electrochem 21:678
3. Spasojevic M, Krstajic N, Jaksic M (1984) J Res Inst Catal Hokkaido Univ 32:29
4. Kotz R, Stucki S (1986) Electrochim Acta 31:1311
5. Hüppauff M, Lengeler B (1993) J Electrochem Soc 140:598
6. Elsen HA, Monson CF, Majda M (2009) J Electrochem Soc 156:F1
7. Hu JM, Zhang JQ, Cao CN (2004) Int J Hydrogen Energy 29:791
8. Velikanova IA, Ivanova NP, Zharskii IM (2008) Russ J Electrochem 44:847
9. Burke LD, Naser NS, Ahern BM (2007) J Solid State Electrochem 11:655
10. Zhang ZX (2000) Titanium electrode technology. Metallurgical Industry Publishing House, Beijing
11. Hutchings R, Muller K, Kotz F, Stucki S (1984) J Mater Sci 19:3987
12. Roginskaya YE, Morozova OV (1995) Electrochim Acta 40:817
13. Benedetti A, Riello P, Battaglin G, Battisti AD, Barbieri A (1994) J Electroanal Chem 376:195
14. Alves VA, Silva LA, Boodts JFC, Trasatti S (1994) Electrochim Acta 39:1585
15. Chen XM, Chen GH (2005) J Electrochem Soc 152:J59
16. Takasu Y, Murakami Y (2000) Electrochim Acta 45:4135
17. Rolewicz J, Comninellis CH, Plattner E, Hinden J (1988) Electrochim Acta 33:573
18. Cardarelli F, Taxil P, Savall A, Comninellis CH, Manoli G, Leclerc O (1998) J Appl Electrochem 28:245
19. Comninellis CH, Vercesi GP (1991) J Appl Electrochem 21:335
20. Kumagai N, Jikihara S, Samata Y, Asami K, Hashimoto K (1993) In: Clayton CR, Hashimoto K (eds) Proceedings of symposium on corrosion, electrochemistry and catalysis of metastable metal and intermetallies. The Electrochem Soc, Pennington
21. Kamegaya Y, Sasaki K, Oguri M, Asaki T, Kobayashi H, Mitamura T (1994) Electrochim Acta 40:889
22. Jiang JF, Xu HB, Wang TY, Wang J, Xu LK, Cheng G (2007) Rare Metal Mat Eng 36:344
23. Sun RX, Xu HB, Wan NF, Wang J (2007) Chem J Chinese Univ 28:904
24. Krysa J, Kule L, Mraz R, Rousar I (1996) J Appl Electrochem 26:999
25. Kim KW, Lee EH, Kim JS, Shin KH, Jung BI (2002) Electrochim Acta 47:2525
26. Endo K, Katayama Y, Miura T, Kishi T (2002) J Appl Electrochem 32:173
27. Mozota J, Conway BE (1983) Electrochim Acta 28:1
28. Warren BE (1996) X-ray diffraction. Addison-Wesley, Reading
29. Otogawa R, Morimitsu M, Matsunaga M (1998) Electrochim Acta 44:1509
30. Sun W, Gong XM, Ye WP, Zhang QY, Zhu XQ (2000) Heat Treat Met 8:13
31. Veprek S (1999) J Vac Sci Technol A 17:2401
32. Li GY, Han ZH, Tian JW, Xu JH, Gu MY (2002) J Vac Sci Technol A 20:674
33. Setoyama M, Nakayama A, Tanaka M, Kitagawa N, Nomura T (1996) Surf Coat Technol 86:225
34. Kim KW, Lee EH, Kim JS, Shin KH, Kim KH (2001) Electrochim Acta 46:915
35. Chen XM, Chen GH, Yue PL (2001) J Phys Chem B 105:4623
36. Pinnow CU, Kasko I, Nagel N, Poppa S, Mikolajick T, Dehm C, Hosler W, Bleyl F, Jahnel F, Seibt M, Geyer U, Samwer K (2002) J Appl Phys 91:9591